THE JOURNAL OF PHYSICAL CHEMISTRY C

Article

Cite This: J. Phys. Chem. C 2019, 123, 16533−16545

pubs.acs.org/JPCC

Light-Induced Electron Paramagnetic Resonance Spectroscopy of Spin-Assisted Charge Transfer in Narrow-Bandgap Copolymer:Methanofullerene Composites

Victor I. Krinichnyi,* Evgeniya I. Yudanova, Nikolay N. Denisov, and Victor R. Bogatyrenko

Department of Kinetics and Catalysis, Institute of Problems of Chemical Physics RAS, Academician Semenov Avenue 1, Chernogolovka 142432, Russia

ABSTRACT: Magnetic resonance, relaxation, and dynamic parameters of polarons and methanofullerene radical anions photoinduced in photovoltaic composites formed by narrow-bandgap poly[(9,9-dioctylfluorenyl-2,7-diyl)-*alt*-(bithiophene)] (F8T2), poly[2,7-(9,9-dioctylfluorene)-*alt*-4,7-bis(thiophen-2-yl)benzo-2,1,3-thiadiazole] (PFO−DBT), and poly[*N*-9′-heptadecanyl-2,7-carbazole-*alt*-5,5-(4′,7′-di-2-thienyl-2′,1′,3′-benzothiadiazole)] (PCDTBT) copolymers as electron donors with [6,6]-phenyl-C_{61}-butanoic acid methyl ester ($PC_{61}BM$) as electron acceptor were comparatively studied by the direct light-induced electron paramagnetic resonance (LEPR) spectroscopy in combination with spectral simulations in a wide temperature range. A number of mobile polarons are captured by deep spin traps formed in bulk heterojunctions due to their disorder. It was shown that the concentration, transport, and recombination of photoinitiated charge carriers depend on the structure of the copolymer matrix and the interaction between the other spin packets, as well as on the number, spatial distribution, and energy depth of the spin traps. The recombination of polarons and methanofullerene radical anions can be described in the framework of a second-order bimolecular process in the F8T2:$PC_{61}BM$ and PFO−DBT:$PC_{61}BM$ composites and a first-order monomolecular process in the PCDTBT:$PC_{61}BM$ bulk heterojunctions. The dependence of the ambipolarity of the copolymer matrix on the anisotropy of spin dynamics is shown.

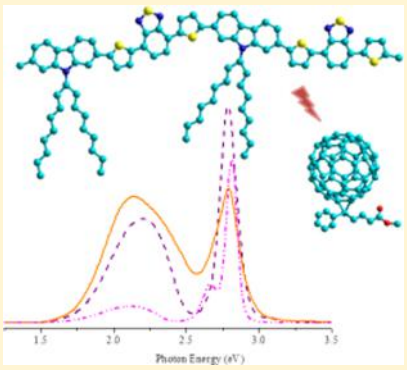

1. INTRODUCTION

Fundamental and applied researches of processes involving spin charge carriers in various molecular materials have been accelerated in the past decade.[1,2] This is due mainly to a possible controlled reorientation of the precession of the electronic spin, which should improve significantly the functionality and efficiency of new molecular electronic and spintronic devices.[3] The electronics properties of such systems are determined by the structure and morphology of their active matrix, as well as by the spin state of the excitations initiated in them. For example, it was proposed to use an organometallic crystal as the active matrix of memory cells of increased capacity, the layers of which are held by van der Waals forces.[4] Information in such a system is planned to record by laser excitation of sedentary interlayer excitons, whose electron and hole are localized on adjacent layers of such molecular crystal. Paramagnetic compounds are also very promising for use as an active material of qubits of quantum computers. Operating with at least a million qubits, such devices will be able to solve a wide range of interdisciplinary problems. This would be possible only by replacing superconducting qubits by cells with controlled orientation of electronic spins.[5] However, the practical use of inorganic crystals is often fraught with fundamental limitations on temperature, their bandgap width, and architecture, and therefore, this requires further investigations. This has led to significant progress in the creation of electronic devices based on bulk organic polymer and copolymer composites with donor and acceptor subgroups. In such systems, the energy of the initiating quanta is conserved as charge-neutral molecular excitations, Frenkel excitons, randomly moving in quasi-one-dimensional (Q1D) chains and quasi-two-dimensional (Q2D) layers of the polymer matrix. Since energy quanta in such structures are absorbed simultaneously by many macromolecules, the dynamics of the corresponding molecular excitation can become coherent. This means that the energy absorbed by such a system can be resonantly transferred to a distance of hundreds of nanometers before exciton dissociation into positive and negative charges. If the nearest macromolecule is located further than this distance, such a process should be accompanied by the irradiation of absorbed energy through phosphorescence or luminescence. When such quasi-particle encounters an electron acceptor, the probability of their dissociation increases sharply. In this case, the electron passes to the acceptor, and the hole remains in the donor phase. If the energy of the donor's lowest unoccupied molecular orbital (LUMO) exceeds that of the acceptor, the separation of oppositely charged charge carriers is significantly accelerated.[6] In some cases, the direction of electron precession of the resulting spin packets can become quantum entangled and

Received: April 11, 2019
Revised: June 13, 2019
Published: June 17, 2019

DOI: 10.1021/acs.jpcc.9b03402
J. Phys. Chem. C 2019, 123, 16533−16545

therefore have different temperatures.[7] Such a spin state can lead to a change in the interaction of both spin reservoirs, the entropy of the entire multispin system, and, finally, the time of their longitudinal and transverse relaxation.

Earlier, poly(3-alkylthiophene) (P3AT) with different alkyl derivatives and [6,6]-phenyl-C_{x1}-butanoic acid ($PC_{x1}BM$, x = 6,7), carbon nanotubes, or graphene were more often used in organic molecular electronic and photonic device prototypes as electron as electron-donating and electron-accepting subgroups, respectively.[8,9] Copolymers with a narrow bandgap were appeared to be more stable and efficient matrix for such purposes.[10] The simplest of them is poly[(9,9-dioctylfluorenyl-2,7-diyl)-*alt*-(bithiophene)] (F8T2) with fluorenyl and bithiophene subgroups as donor and acceptor subgroups, respectively. Relatively low ability of acceptance of an electron by bithiophene group caused direct photoinitiation of polarons on chains of the F8T2:$PC_{71}BM$ composite backbone.[11] Ambipolar poly[2,7-(9,9-dioctylfluorene)-*alt*-4,7-bis(thiophen-2-yl)-benzo-2,1,3-thiadiazole] (PFO−DBT) is more frequently used as the active matrix in molecular electronics. It occurs mainly because the adding of DBT subunits to the bithiophene groups during the transition from F8T2 to PFO−DBT narrows the bandgap of the latter matrix[12] and increases the probability of intramolecular charge hopping from the fluorene groups to DBT subunits.[13] Under illumination, the latter act as traps of excitons that increases an ambipolarity of respective composite. Intrachain energy transfer along the chains of PFO−DBT becomes more effective in comparison with interchain charge hopping, thereby considerably increasing efficiency of the corresponding polymer photovoltaic and light-emitting devices.[14] Significant improvement of electronic properties of photovoltaic elements was reached when using in them poly[*N*-9′-heptadecanyl-2,7-carbazole-*alt*-5,5-(4′,7′-di-2-thienyl-2′,1′,3′-benzothiadiazole)] (PCDTBT) with carbazole and benzothiadiazole groups as electron donor and acceptor, respectively.[15] This allowed creating, e.g., 2.7-carbazole-based copolymer solar batteries with the power conversion efficiency more than 7%,[16,17] and field transistors with mobility of charge carriers near 17 $cm^2/(V\ s)$.[18] A wide spatial delocalization of excitons in such narrow-bandgap systems should result in superfast charge separation. However, experimental data indicated discrepancy of observed transfer rate of an electron and too slow migration of an exciton. Therefore, the assumption[19,20] was made that the increased quantum yield in the PCDTBT:$PC_{x1}BM$ and other similar nanocomposites could be due to their layered morphology and reduced spin delocalization over a polaron that decreases the probability of charge recombination.

Excitation of electron−hole pairs by the polarized infrared irradiation in an inorganic layered ordered lattice induces reorientation of the photoexcited pseudospins for several attoseconds.[21] This effect can possibly be used for creation of superfast computers with optical clock frequencies based on the specified copolymer composites. Earlier it was shown[4] that illumination of inorganic bilayered ordered compounds initiates the formation in their bulk of intralayered and interlayered excitons. Both the charges of intralayered excitons are formed in each layer of a composite while free electrons and holes of interlayered excitons are located on its neighboring layers. The assumption of a possibility of formation of such excitons in the above mention Q2D organic copolymer composites would be quite logical. In contrast to inorganic systems, so organized compounds should be better materials for molecular electronics, mainly due to their low spin−orbit interactions and their ability to be integrated in hybrid organic−inorganic devices.[22−24] Charge separation in the narrow-bandgap polymer systems happens mainly during ∼0.1 ns, therefore one may to expect that the excitation caused by the $\pi-\pi^*$ interband transition reaches a border of a bulk heterojunctions (BHJ) on which such separation is carried out before it becomes spatially localized and collapsed into an exciton. Therefore, neither diffusion process no binding energy of excitons should not influence superfast charge transfer in such systems. It has to be defined rather by an ambipolarity of copolymer matrix whose acceptor group has a greater influence on electronic, optical and electrochemical properties of such compounds.[25−27] This allows handling the main functional properties of molecular devices by variation of structure of acceptor group. Thus, in order to create molecular electronic, spintronic, and photonic elements of a new generation it would be important first to determine the influence of the structure, morphology of the active matrix, and the spin state of excitations on the electron-dynamic properties of polymer systems. However, despite the high prospects of using copolymer composites in molecular electronics, no exact correlations of the structure and morphology of such compounds with their basic electronic and energy properties have been obtained yet.

The principal important is the fact that dissociation of excitons leads to formation of two spin ensembles with opposite charges, namely radical pairs in BHJ of copolymer composites[28,29] and/or biradicaloids in their ambipolar matrices.[30] The efficiency and functionality of the above systems can be governed mainly by exchange interaction and a recombination of free charge carriers formed in them. The order of a recombination process depends on the main parameters of spin traps formed in a system due to its disordering. It can be defined from the analysis of delay of paramagnetic susceptibility after switching off the initiating irradiation.[31,32] Different methods can be used for the study of such organic systems, e.g., femtosecond time-resolved optically detected[11] and absorption-detected[28] magnetic resonance methods. However, they are indirect methods able only register an effective concentration of the carriers formed in result of their fast forward initiation and slow reversed recombination upon continuous irradiation of respective BHJ. It limits the use all the advantages of the method for studying complex processes occurring in multispin polymer systems necessary for creation of novel molecular elements. Because the most charge carriers formed in organic semiconductors possess spin, their formation, dynamics, and recombination become spin-dependent.[28] This makes it possible to handle the relaxation and electronic properties of such systems by changing the state of their spin ensembles. The spin nature of charge carriers formed in these systems provides an unique opportunity to use the direct method of electron paramagnetic resonance (EPR) spectroscopy for detecting and detailed study of all spin-assisted processes occurring in these compounds.[28,33] Besides this, coherent magnetic resonance control of spin states in organic systems with spin charge carriers can significantly improve their electronic parameters and create novel, more functional molecular devices.

Organic systems are mainly studied by continuous wave (cw) and various pulse (spin−echo, ENDOR, TRIPLE, *etc.*) EPR techniques.[34] The pulse methods are suitable to obtain

DOI: 10.1021/acs.jpcc.9b03402
J. Phys. Chem. C 2019, 123, 16533−16545

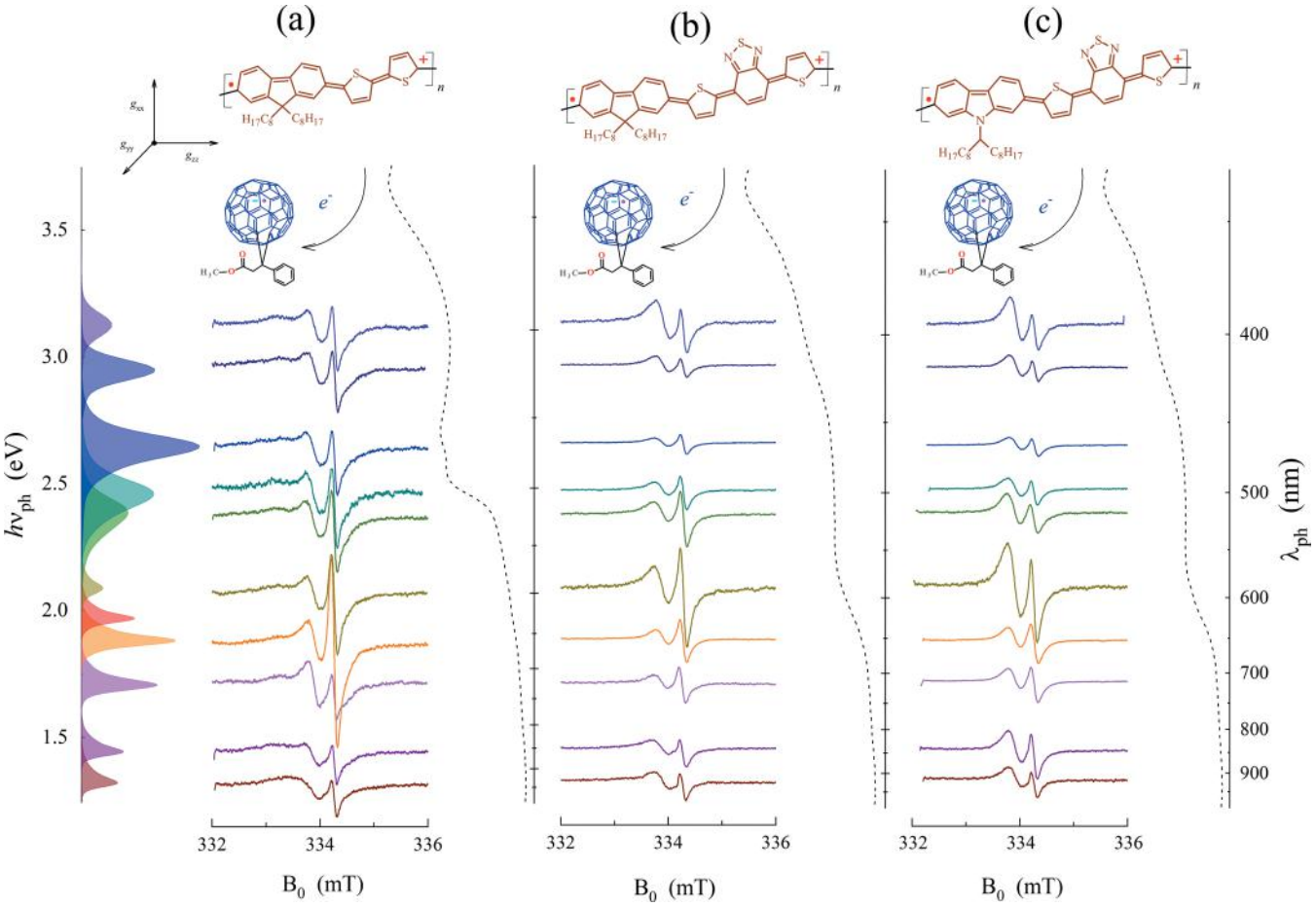

Figure 1. X-band (9.7 GHz/340 mT) LEPR spectra of nanocomposites formed by the F8T2 (a), PFO−DBT (b), and PCDTBT (c) copolymers with the $PC_{61}BM$ molecules and background initiated at T = 77 K by monochromatic light sources with different photon energy $h\nu_{ph}$ normalized to the luminous emittance of the light sources I_l(solid lines) and their respective NIR−Vis−UV absorption spectra (dashed lines) obtained at T = 298 K. Left translucent filled lines show irradiation spectra of the light sources normalized to their luminous emittance I_l. In the top, the structures of copolymer:methanofullerene BHJ formed in respective nanocomposites are shown schematically. The transfer of an elementary negative charge from copolymer chain to methanofullerene molecule accompanied by the formation on the former of polaron $P^{+\bullet}$(hole)with an elementary positive charge and spin $S = {}^1/_2$ is shown as well. The spin of is normally localized over a larger ($n \geq 3$) number of copolymer monomers occupied by a polaron than shown in the figure. The orientation of the principal axes of the polaron's ***g***-tensor is also given.

spin distribution over topological centers exciting in such objects under various physical influences. However, they often provide ambiguous results concerning spin coupling, relaxation, and dynamics in some conjugated polymers[35−37] and polymer:fullerene composites.[38,39] Some limitations can be passed by the study of polymer systems at different frequencies of spin precession and lowered temperatures.[36,37,40] Because the recording and interpretation of pulse EPR spectra requires sophisticated technical equipment and a more advanced theoretical background, direct cw EPR spectroscopy is widely used for the study of spin ensembles in conjugated polymers and their nanocomposites. The main significant advantages of the cw EPR spectroscopy with respect to the pulse magnetic resonance methods are the higher sensitivity to paramagnetic species with different mobility in a wide range of electron relaxation, spin precession frequency and temperature. So, the light-induced cw EPR (LEPR) spectroscopy became one of the most powerful method used for the study of all spin-assisted processes carrying out in polymer:fullerene systems.[28,41,42] It was appeared to be able to detect directly all the stages of the formation, motion and recombination of spin charge carriers. Indeed, the number of photoinitiated quasi-pairs of charge carriers can be determined by the "light on-light off" method using comparison of EPR and LEPR spectra before and after light illumination. Because both the polaron and the fullerene radical anion possess the spin $S = {}^1/_2$ and weakly anisotropic *g*-factors, they demonstrate at the often-used X-band EPR partly overlapping doublet of their contributions. This method was used for the study of the main magnetic resonance parameters of spin charge carriers photoinitiated in some organic polymer and copolymer composites.[20,30,43−49] A preliminary cw EPR study of some copolymer composites[50−54] allowed to determine the main values of magnetic resonance parameters of charge carriers and to identify some correlations of their spin state and dynamic properties with the structure and morphology of such systems. It was demonstrated the capture of a part of mobile polarons by high-energetic spin traps formed due to structural disordering of their matrices. The number, spatial distribution, and energy depth of such traps depend on the structure and morphology of the composites. A sufficient dependence of the magnetic resonance, relaxation, and dynamic parameters of spin charge carriers on their number and exchange coupling, as well as on the energy of initiating photons, was also shown.

DOI: 10.1021/acs.jpcc.9b03402
J. Phys. Chem. C 2019, 123, 16533−16545

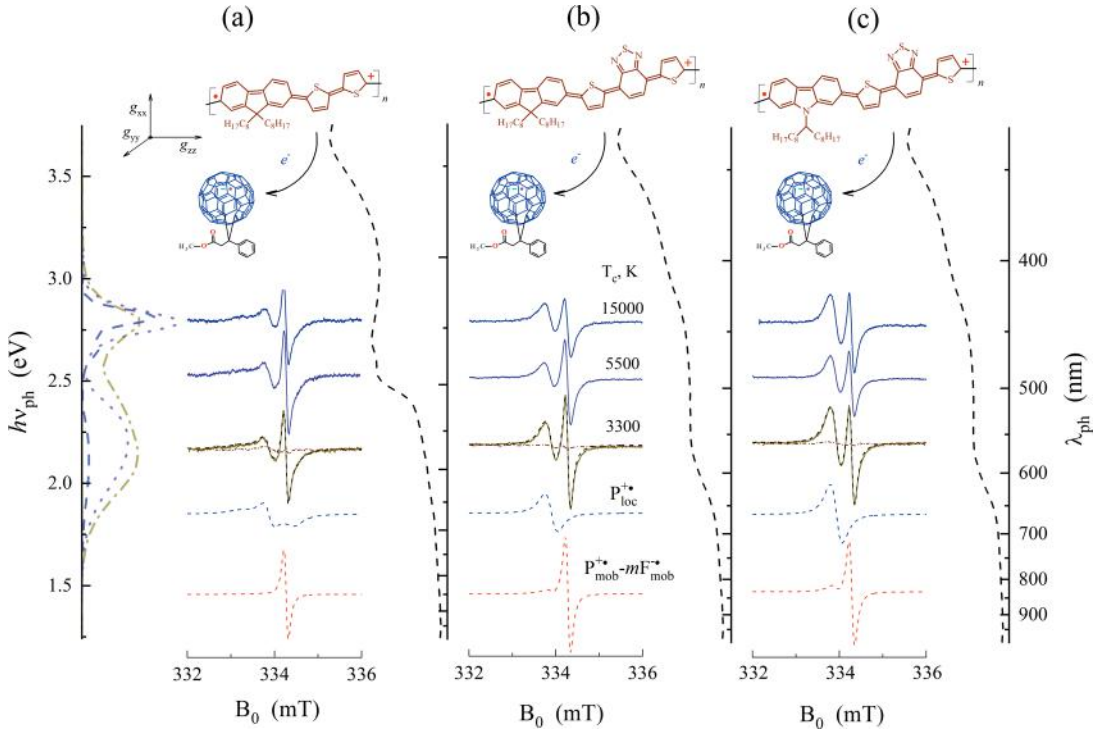

Figure 2. X-band (9.7 GHz/340 mT) LEPR spectra of charge carriers background initiated by achromatic, white light with CCT of T_c = 15000, 5500, and 3300 at 77 K in BHJ formed by the F8T2 (a), PFO−DBT (b), and PCDTBT (c) copolymers with the $PC_{61}BM$ molecules normalized to the luminous emittance of the light sources I_l (solid lines) and their respective NIR−Vis−UV absorption spectra (dashed lines) obtained at T = 298 K. By the dashed lines are shown theoretically calculated Lorentzian effective LEPR spectra and their contributions caused by localized polarons $P^{+\bullet}_{loc}$ and highly mobilized radical pairs, $P^{+\bullet}_{mob} \leftrightarrow mF^{-\bullet}_{mob}$ well fitting the experimental LEPR spectra with the parameters presented in Table 1. Left dashed, dotted, and dash-dotted lines show irradiation spectra of the light sources with CCT of T_c = 15000, 5500, and 3300 K, respectively, normalized to their luminous emittance I_l. In the top, the structures of copolymer:methanofullerene BHJ formed in respective nanocomposites are shown schematically. The transfer of an elementary negative charge from copolymer chain to methanofullerene molecule accompanied by the formation on the former of polaron $P^{+\bullet}$(hole) with an elementary positive charge and spin $S = {}^1/_2$ is shown as well. The spin of is normally localized over a larger ($n \geq 3$) number of copolymer monomers occupied by a polaron than shown in the figure. The orientation of the principal axes of the polaron's g-tensor is also given.

In this paper, we report the results of a detailed comparative cw LEPR study of the formation, relaxation, dynamics, and recombination of charge carriers, photoinduced in the narrow-bandgap F8T2:$PC_{61}BM$, PFO−DBT:$PC_{61}BM$, and PCDTBT:$PC_{61}BM$ BHJ. The use of the method in combination with spectral simulations allowed us to obtain the correlations of the magnetic, relaxation, dynamics, and recombination parameters of spin charge carriers photo-induced in these compounds with the structure of the composites in a wide temperature range. The data obtained were compared with those determined by the optical absorption method.

II. EXPERIMENTAL SECTION

2.1. Ingredients Used in Experiments. In the work, poly[(9,9-dioctylfluorenyl-2,7-diyl)-*alt*-(bithiophene)] (F8T2) manufactured by American Dye Source, Inc., USA, poly[2,7-(9,9-dioctylfluorene)-*alt*-4,7-bis(thiophen-2-yl)benzo-2,1,3-thiadiazole] (PFO−DBT) distributed by Sigma-Aldrich, The Netherlands, and poly[*N*-9′-heptadecanyl-2,7-carbazole-*alt*-5,5-(4′,7′-di-2-thienyl-2′,1′,3′-benzothiadiazole)] (PCDTBT) distributed by Sigma-Aldrich, The Netherlands, were used as electron donors. [6,6]-phenyl-C_{61}-butanoic acid methyl ester ($PC_{61}BM$) distributed by Solenne BV, The Netherlands was used as an electron acceptor. The chemical structures of these components are shown schematically in Figure 1 and Figure 2.

2.2. Preparation of Copolymer:Methanofullerene Composites. All the samples were prepared as following. First 1.4 mg of each copolymer was dissolved in 1 mL of dichlorobenzene, treated inside the 50 W ultrasonic cleaner DADI DA-968 for 10 min, and heated for 30 min at T = 333 K with the following ultrasonic treatment for 10 min until its complete dilution. Then 5.6 mg of $PC_{61}BM$ was added into 1 mL of these so-treated solutions followed their heating for 2.5 h at T = 333 K and then held at room temperature for 20 h. Finally, 30 μL of the resulting solutions were cast by 5 μL drops into both sites of thin ceramic plate and dried until the samples were formed as double-sided films of nearly 4 × 8 mm^2 in size and nearly 0.1 mm in thickness. In order to avoid a contact of the sample with the water and air, all manipulations were performed in a dry inert atmosphere.

2.3. NIR−Vis−UV Absorption Spectra of Copolymer Composites. Optical absorption spectra of the composites' films were obtained by using spectrophotometer Specord-250 plus (Analytik Jena) at their scanning within the band 1.13−6.53 eV (1100−190 nm) at T = 298 K. They are shown in Figure 1 and Figure 2. The composition and positions of the spectral components were determined accurately by differentiating the initial absorption spectra.

2.4. Photoinitiation of Spin Charge Carriers. The samples were irradiated directly in the EPR cavity of the spectrometer trough the quartz cylindrical light guide by 5 W

DOI: 10.1021/acs.jpcc.9b03402
J. Phys. Chem. C 2019, 123, 16533−16545

Luxeon LED monochromatic sources with the photon energy $h\nu_{ph}$/wavelength λ_{ph}/luminous emittance I_l of 1.32 eV/940 nm/750 lx, 1.46 eV/850 nm/870 lx, 1.61 eV/770 nm/1160 lx, 1.88 eV/660 nm/1950 lx, 1.97 eV/630 nm/1110 lx, 2.10 eV/590 nm/450 lx, 2.34 eV/530 nm/960 lx, 2.48 eV/500 nm/1500 lx, 2.64 eV/470 nm/2450 lx, 2.95 eV/420 nm/1520 lx, and 3.14 eV/395 nm/630 lx as well as achromatic, white sources with the correlated color temperature (CCT) of T_c = 15000, 5500, and 3300 K and luminous emittance I_l = 3020, 4000, and 2480 lx, respectively. The I_l values of the sources were determined using the IMO-2N broadband bolometric light emission power meter and LX-1010BS digital luxmeter and were used to further normalize the number of spins photoinitiated in the samples under study.

2.5. LEPR Spectra Measurements and Processing. CW EPR measurements were performed using X-band (3 cm, 9.7 GHz) PS-100.X spectrometer with a maximum microwave power of 150 mW and 100 kHz synchronous/phase detection. Dark and photoinduced EPR spectra of the copolymer:methanofullerene nanocomposites were obtained at 77 K when they were inserted into a quartz Dewar filled with liquid nitrogen and placed into the EPR spectrometer cavity. For EPR measurements at higher temperatures (T = 90−320 K), the samples were situated in a quartz flow Dewar cell in a stream of dry nitrogen, whose temperature was stabilized by the BRT SKB IOC controller, equipped with a platinum temperature sensor Pt100. The signal-to-noise ratio of signals was improved by its accumulation during multiple scanning of the EPR spectra. The processing and simulation of the spectra were performed using the EasySpin and OriginLab programs. The relative concentrations of both the spin charge carriers stabilized in darkened and illuminated samples were determined separately from the comparison of EPR and LEPR spectra registered far from their microwave saturation (the "light on-light off" method) followed by their deconvolution, as described earlier.[20,44,47] Landé g-factor of spin charge carriers was determined using the *N*,*N*-diphenyl-*N*′-picrylhydrazyl (DPPH) standard with g = 2.0036 ± 0.0002.[55] The accuracy of estimating the intensity I, g-factor of the line and the distance between its positive and negative spectral peaks ΔB_{pp} was determined to be 1.5%, $\pm 2 \times 10^{-4}$ and $\pm(1-4) \times 10^{-3}$ mT, respectively. The times of spin−lattice T_1 and spin−spin T_2 relaxation of spin ensembles were determined using the steady-state microwave saturation method,[56] adapted for the study of spin pairs photoinitiated in organic polymer:fullerene nanocomposites.[57]

3. RESULTS AND DISCUSSION

3.1. NIR−Vis−UV Absorption Spectra of Copolymer Composites. Normally, optics absorption spectra of the narrow-band composites consist of the visible Q-band contribution due to copolymer and the Soret (B-band) contribution due to the presence in the composite of the fullerene globes.[14,58] Q-band term is originated by the $\pi-\pi^*$ transition between respective bonding and antibonding molecular orbitals of respective polymer.[59,60] Intra- and intermolecular interactions in the composites split these contributions into two and three components, respectively. The splitting of both the spectral components can also be due to interactions of respective subunits with own microenvironment.

The F8T2:PC_{61}BM, PFO−DBT:PC_{61}BM, and PCDTBT:PC_{61}BM composites demonstrate triple B-band spectra registered at 339, 268, 218 nm (3.66, 4.63, 5.69 eV); 338, 268, 219 nm (3.67, 4.63, 5.66 eV); and 339, 269, 221 nm (3.66, 4.61, 5.61 eV), respectively (shown in Figure 1 and Figure 2 without the both highest energetic peaks). These values lie near 329, 257, and 213 nm (3.77, 4.82, and 5.82 eV), obtained for the pure C_{60} molecules.[61] The Q-band contribution of the F8T2:PC_{61}BM composite consists of two peaks registered at 496 and 461 nm (2.50 and 2.69 eV) which lie near those obtained for analogous systems.[11,62] Unlike the F8T2:PC_{61}BM compound, the PFO−DBT:PC_{61}BM composite demonstrates two Q-band double lines (Figure 2). Their terms recorded at 608 and 571 nm (2.04 and 2.17 eV) as well as 415 and 397 nm (2.99 and 3.12 eV) can be attributed to the benzothiadiazole and fluorine subunits, respectively.[63,64] The absorption spectrum of the PCDTBT:PC_{61}BM film is generally similar to that of the PFO−DBT:PC_{61}BM composite. Its PCDTBT content is characterized by two Q-band double lines, registered at 610 and 569 nm (2.03 and 2.18 eV) as well as 416 and 397 nm (2.98 and 3.12 eV). They can be attributed to the benzothiadiazole and carbazole subunits, respectively.[65,66]

Analysis of the results obtained allows us to expect an increase in the structural ordering and ambipolarity in the F8T2 → PFO−DBT → PCDTBT series, which determine the electronic properties of the corresponding of narrow-bandgap copolymer composites.

3.2. LEPR Spectra Composition and Magnetic Resonance Parameters. Figure 1 shows the LEPR spectra of paramagnetic centers photoinduced in the F8T2:PC_{61}BM, PFO−DBT:PC_{61}BM, and PCDTBT:PC_{61}BM composites by monochrome light sources of different photon energies. LEPR spectra of these samples registered upon their irradiation by white light sources with correlated color temperatures, T_c = 15000, 5500, and 3300 K are shown in Figure 2. As in the case of other similar compounds,[47,49] the low-field and high-field components of these spectra were assigned to polarons P^+ formed on the copolymer chains, as well as to the methanofullerene radical anions $mF^{-\bullet}$, situated between the corresponding macromolecules, respectively. It can be seen from the Figures that the relative contributions of these charge carriers are determined by the structure of the compounds, as well as by the luminancem I_l, and CCT, T_c, of the light sources.

Previously, it was shown[51−54] that the shape and intensity of the LEPR spectra of organic photovoltaic systems depend also on the energy of the initiating photons and on the properties of the radical microenvironment. Some charge carriers may be captured by deep spin traps formed in organic composites due to the disordering of their polymer matrices. When a composite is irradiated with photons of certain energy, some deeply trapped polarons can be released, so then the number of mobile carriers should be increased. This leads to variations in the spin composition, effective paramagnetic susceptibility, and interaction between spin ensembles in such systems. An exchange coupling of the mobile and trapped charge carriers changes additionally the total paramagnetic susceptibility of the systems and, therefore, their spin-dependent magnetic resonance, relaxation, and dynamic parameters. Normally, polarons stabilized and/or initiated in conjugated polymers demonstrate a weak anisotropy of their g-factor.[47,49] Since spin charge carriers in photovoltaic systems are also characterized by a weak anisotropy of their magnetic parameters,[48] their effective LEPR spectra should also be changed by the capture of a part of charge carriers by deep spin traps. Besides, in some cases, polarons can combine to form interchain pairs of mobile

DOI: 10.1021/acs.jpcc.9b03402
J. Phys. Chem. C 2019, 123, 16533−16545

Table 1. Isotropic g-Factor of Polarons g^{P}_{iso}, Peak-to-Peak Line Width of Polarons ΔB^{P}_{pp} and Methanofullerene Radical Anions ΔB^{mF}_{pp}, Concentration Ratio of Mobile Methanofullerene Radical Anions to That of Localized Polarons n^{mF}_{mob}/n^{P}_{loc}, Spin−Lattice and Spin−Spin Relaxation Times of Polarons, T^{P}_{1} and T^{P}_{2}, Respectively, Methanofullerene, T^{mF}_{1} and T^{mF}_{2}, Respectively, Evaluated from Their LEPR Lineshapes, Coefficients of Polaron Diffusion along, D^{P}_{1D}, and Between, D^{P}_{3D}, Copolymer Chains, and Methanofullerene Libration Dynamics near the Main Molecular Axis D^{mF}_{lb}, Determined under Continual Illumination of the Composites by Achromatic, White Light with Different Correlated Color Temperature, T_c at T = 77 K

	F8T2:$PC_{61}BM$			PFO−DBT:$PC_{61}BM$			PCDTBT:$PC_{61}BM$		
parameter	T_c = 15000 K	T_c = 5500 K	T_c = 3300 K	T_c = 15000 K	T_c = 5500 K	T_c = 3300 K	T_c = 15000 K	T_c = 5500 K	T_c = 3300 K
g^{P}_{iso}	2.002_{22}	2.002_{27}	2.002_{34}	2.002_{26}	2.002_{37}	2.002_{28}	2.002_{07}	2.002_{09}	2.002_{05}
ΔB^{P}_{pp}, mT	0.289	0.297	0.317	0.217	0.218	0.228	0.210	0.205	0.208
ΔB^{mF}_{pp}, mT	0.103	0.107	0.105	0.124	0.132	0.125	0.125	0.140	0.129
n^{mF}_{mob}/n^{P}_{loc}	0.113	0.097	0.077	0.731	0.924	0.555	0.469	1.010	0.715
T^{P}_{1}, s	1.37×10^{-6}	8.46×10^{-7}	1.23×10^{-6}	1.32×10^{-6}	2.45×10^{-6}	1.46×10^{-6}	2.08×10^{-6}	7.53×10^{-7}	2.04×10^{-6}
T^{P}_{2}, s	2.27×10^{-8}	2.21×10^{-8}	2.07×10^{-8}	3.02×10^{-8}	3.01×10^{-8}	2.88×10^{-8}	3.12×10^{-8}	3.19×10^{-8}	3.15×10^{-8}
T^{mF}_{1}, s	1.04×10^{-6}	6.33×10^{-7}	1.03×10^{-6}	5.92×10^{-7}	7.41×10^{-7}	5.23×10^{-7}	1.11×10^{-6}	4.37×10^{-7}	4.35×10^{-7}
T^{mF}_{2}, s	6.35×10^{-8}	6.13×10^{-8}	6.26×10^{-8}	5.29×10^{-8}	4.99×10^{-8}	5.27×10^{-6}	5.25×10^{-8}	4.68×10^{-8}	5.08×10^{-8}
D^{P}_{1D}, rad/s	6.20×10^{11}	2.93×10^{11}	4.99×10^{11}	1.20×10^{12}	4.69×10^{12}	1.37×10^{12}	2.74×10^{12}	4.51×10^{11}	2.84×10^{12}
D^{P}_{3D}, rad/s	2.68×10^{6}	6.75×10^{6}	2.77×10^{6}	5.18×10^{6}	1.47×10^{6}	3.79×10^{6}	2.21×10^{6}	1.83×10^{7}	2.32×10^{6}
D^{mF}_{lb}, rad/s	7.24×10^{10}	1.03×10^{11}	1.23×10^{11}	2.96×10^{10}	1.63×10^{10}	4.59×10^{10}	1.94×10^{10}	2.68×10^{10}	4.94×10^{10}

diamagnetic $P^{+\bullet}_{mob} \leftrightarrow P^{+\bullet}_{mob}$ or localized paramagnetic $P^{-\bullet}_{loc} \leftrightarrow P^{+\bullet}_{loc}$ bipolarons with equal g-factors.[67,68] Therefore, to determine correctly the composition, magnetic, and dynamic parameters of all paramagnetic centers, photoinitiated in the composites under study, as well as to analyze changes in these parameters due to the influence of various factors, their effective LEPR spectra should be deconvoluted as in the case of other similar systems.[44,47−49] This procedure allowed us to obtain separately the main magnetic resonance parameters of all spin packets and analyze their dependence, for example, on the properties of the samples during their irradiation and/or heating.

Figure 2 depicts the total LEPR spectra and their terms due to the polarons captured by spin traps $P^{+\bullet}_{loc}$ and also pairs of mobile charge carriers, $P^{+\bullet}_{mob} \leftrightarrow mF^{-\bullet}_{mob}$ in the samples illuminated by white light with the CCT of T_c = 5500 K. The fitting of effective spectra showed the absence in all composites of methanofullerene radical anions $mF^{-\bullet}_{loc}$, which presents in some other polymer:fullerene composites.[47] This may be evidence of the formation of a smaller number of deep spin traps in the more structured composites studied. The isotropic Landé g-factor of methanofullerene radical ions was determined to be $g^{mF}_{iso} = 1.999_{89}$ that corresponds to $g^{mF}_{iso} = 1.9994_{8}$[44] and $g^{mF}_{iso} = 1.999_{87}$,[20,48] determined at millimeter ($\omega_e/2\pi$ = 130 GHz) waveband EPR. The isotropic g-factors of polarons photoinitiated by white light in the F8T2:$PC_{61}BM$, PFO−DBT:$PC_{61}BM$, and PCDTBT:$PC_{61}BM$ composites are summarized in Table 1. These values correspond to $g^{P}_{iso} = 2.002_{47}−2.003_{30}$, obtained for polaronic charge carriers in similar photovoltaic systems.[20,47,48]

3.3. Spin Susceptibility. It was shown previously[51−53] that the number and composition of the spin charge carriers, formed in F8T2:$PC_{61}BM$, PFO−DBT:$PC_{61}BM$, and PCDTBT:$PC_{61}BM$ BHJ as a result of exciton dissociation are determined by their structure as well as by the density and the energy of the initiating light photons. Some mobile spin charge carriers are separated in these BHJ, leave them, and reach the corresponding electrodes, while their other part tends to recombine. This causes the simultaneous occurrence at the phase boundary of two oppositely directed processes of the appearance and pairing of spins. The balance of such processes depends on the spatial density and energy depth of the spin traps formed in disordered polymer matrices and determines the number of spin charge carriers able to reach the electrodes. It is proportional to the ratio of mobile charge carriers and their part captured by spin traps, n^{P}_{mob}/n^{P}_{loc} or n^{mF}_{mob}/n^{P}_{loc}. This concentration ratio is frequency-dependent. The probability of an interaction between individual spin ensembles in an ordered system follows the law $p_{cr} = 2\pi\sqrt{M_2}\exp(-\omega_e^2/8\pi^2M_2)$, where M_2 is second moment of a spectrum. At the high ω_e, spin−spin interaction decreases strongly, spin ensembles become noninteracting and therefore can be saturated at lower amplitude of the magnetic term B_1 of microwave polarizing field. Indeed, the analysis of the data obtained by multifrequency LEPR study, e.g., of the P3HT:$PC_{61}BM$ BHJ,[20,43,69,70] showed that such effect forces the above concentration ratio to follow the law $n^{P}_{mob}/n^{P}_{loc} = n^{mF}_{mob}/n^{P}_{loc} = 9.52 \times 10^{-5}\sqrt{k_2}\exp(-\omega_e^2/8\pi^2k_2)$ with $k_2 = 1.19 \times 10^{9}$ s^{-2}. This parameter seems quite obvious to be governed also by spin interaction with the lattice phonons.

Figure 3 depicts the temperature dependences of the number of localized polarons $P^{+\bullet}_{loc}$, mobile methanofullerene radical anions $mF^{-\bullet}_{mob}$ (inset), and also the ratio of their concentrations, n^{mF}_{mob}/n^{P}_{loc}, photoinitiated in the composites under study by photons of white light with CCT of 5500 K. From the figure it can be seen that the number of polarons captured by spin traps in the F8T2:$PC_{61}BM$ and PCDTBT:$PC_{61}BM$ BHJ varies little with temperature. On the other hand, these centers photoinduced in the PFO−DBT:$PC_{61}BM$ BHJ demonstrate an extreme temperature dependence with a characteristic point around $T \approx 120$ K. As in the case of other polymer systems, this dependence can be caused by a collective change in the diffusion rate of spin charge carriers, by their coupling with other spin packets, and also by the dissociation of some diamagnetic bipolarons into polaron pairs.[68,71,72] The possible capture of a part of polarons by spin traps and the release of their parts under the light illumination[51−54] should also be taken into account. The data obtained show that as the composites are heated up to the above characteristic temperature, the number of mobile charge carriers, as well as the corresponding parameter n^{mF}_{mob}/n^{P}_{loc} decreases significantly, possible due to the acceleration of recombination of mobile charge carriers. However, it should be noted a larger concentration of mobile charge carriers

DOI: 10.1021/acs.jpcc.9b03402
J. Phys. Chem. C 2019, 123, 16533−16545

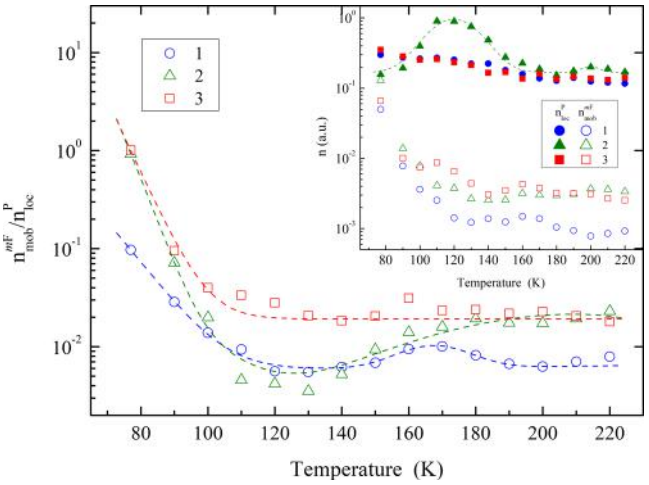

Figure 3. Temperature dependence of the number of localized $P^{+\bullet}_{loc}$ polarons and mobile methanofullerene radical anions $mF^{-\bullet}_{mob}$ (filled and open points, respectively, in the inset), induced in the F8T2:$PC_{61}BM$ (1), PFO−DBT:$PC_{61}BM$ (2), and PCDTBT:$PC_{61}BM$ (3) composites by achromatic/white light source with the color temperature T_c = 5500 K as well as the ratio of their concentrations, n^{mF}_{mob}/n^{P}_{loc}. The lines are drawn arbitrarily only for illustration to guide the eye.

photoinduced in the PCDTBT:$PC_{61}BM$ composite in the entire temperature range (see Figure 3). This may be due to the better ordering of its copolymer matrix and a more optimal mechanism of the dissociation of the initial excitons into free charge carriers.[15,73]

3.4. Recombination of Spin Charge Carriers. When the lighting is turned off, the spin charge carriers begin to recombine, which leads to a decrease in their concentration and the intensity of appropriate LEPR spectrum. This process should depend on the structure, morphology, and ordering of a composite, as well as on the dynamics and spin state of photoinitiated charge carriers. The simplest first-order mechanism is characteristic of recombination of radical pairs formed from the initial unseparated excitons. If a polaron with the positive charge leaves such a pair, it will be able to recombine with are mote methanofullerene radical anion located between the copolymer layers. If the fullerene radical anion does not interact with the encountered polaron, the duration of their collisions should be determined by the dynamics of the latter. Such a recombination process becomes bimolecular and should follow a second order. This parameter obtained for the F8T2:$PC_{61}BM$, PFO−DBT:$PC_{61}BM$, and PCDTBT:$PC_{61}BM$ composites appeared to be 2.23, 2.25, and 1.23, respectively.[51−54] The key role in recombination of spin charge carriers should play their dynamics and exchange interaction, as well as the formation of spin traps in copolymer backbone. So, a different mechanism of charge recombination may indicate a difference not only in their structural ordering but also in spatial distribution and energetic depth of the spin traps in these systems. In this case, the polaron can either be captured by a vacant trap or recombine with the nearest oppositely charged radical anion. Multiple sequent captures and releases of polarons reduce their energy, which finally leads to their localization in the deepest spin traps and, consequently, to an increase in the concentration of localized carriers over time. The recombination of spin charge carriers in a polymer system with energetically different spin traps should follow the law[31]

$$\frac{n(t)}{n_0} = \frac{\pi\epsilon\delta(1+\epsilon)\nu_d}{\sin(\pi\epsilon)}t^{-\epsilon} \quad (1)$$

where $\epsilon = k_BT/E_0$, k_B is Boltzmann constant, E_0 is distribution of the trap energy, δ is the γ function, and ν_d is the attempt jump frequency for polaron detrapping.

The fitting of the effective LEPR spectra shown in Figure 2 allowed us to analyze separately decay processes of both spin charge carriers photoinitiated in the polymer system under study. Figure 4 shows the decries in an initial concentrations of

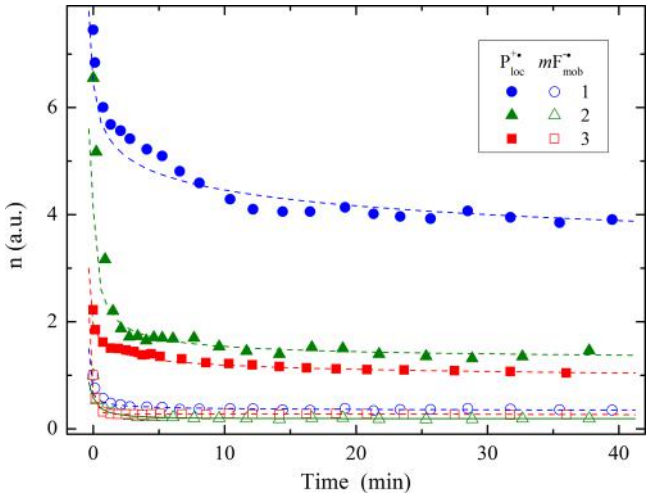

Figure 4. Dependences of the decay of the polaron and methanofullerene charge carriers initiated in the F8T2:$PC_{61}BM$ (1), PFO−DBT:$PC_{61}BM$ (2), and PCDTBT:$PC_{61}BM$ (3) composites by an achromatic, white light source with CCT of T_c = 5500 K at T = 77 K. Dashed lines show the dependences calculated from 1 with respective E^P_0 and E^{mF}_0 values presented in Table 1. The data obtained are normalized to the concentration of mobile methanofullerene radical anions.

both charge carriers photoinitiated in the composites under study once the white light source with a CCT of 5500 K was turned off. It is seen from Figure 4, that the experimental data obtained for the F8T2:$PC_{61}BM$, PFO−DBT:$PC_{61}BM$, and PCDTBT:$PC_{61}BM$ composites can be well fitted by 1 with E^P_0 = 0.049_1 and E^{mF}_0 = 0.013_2 eV, E^P_0 = 0.010_6 and E^{mF}_0 = 0.010_2 eV, and E^P_0 = 0.027_7 and E^{mF}_0= 0.004_6 eV, respectively. Some deviation in the fitting made for polaron decay in the former composite can occur due to the possible prevalence in experimental dependence of the persistent component over the prompt one observed in other polymer:fullerene composites.[67] It is also seen from the analysis of the data that the E^{mF}_0 parameter decreased monotonically at the replacement of the F8T2 backbone by the PFO−DBT one and then by the PCDTBT matrix. At these serial transitions, the E^P_0 parameter first decreases significantly, and then increases almost to its initial value. Such a variation occurs antibathically with a change in the anisotropy of the polaron dynamics described below. Thus, the recombination of long-lived localized polarons $P^{+\bullet}_{loc}$ and mobile methanofullerene radical anions $mF^{-\bullet}_{mob}$ formed from the initial excitons can indeed be described within the framework of the above model that properly takes into account the number, energy depth, and

DOI: 10.1021/acs.jpcc.9b03402
J. Phys. Chem. C 2019, 123, 16533−16545

spatial distribution of spin traps formed in disordered copolymer backbone.

3.5. LEPR Line Width. The shape and width of the LEPR line are the other important parameters reflecting the spin-assisted processes occurring in polymer systems.[28] They reflect the interaction between spin ensembles and their distribution in the composite bulk, which should be taken into account when analyzing their spectral lines. Regular or chaotic distribution of the spins in a solids causes a Gaussian or Lorentzian line shape, respectively, and an additional line broadening proportional to their concentration n.[74] The interaction between different spin packets in real systems initiates the appearance of a more complex line with the superposition/convolution of the Lorentzian and Gaussian distribution functions. For example, Gaussian contribution in LEPR spectra of structurally close organic composites can be increased due to a hyperfine interaction of photoinitiated spin charge carriers with own microenvironment.[48] So, from the analysis of experimental LEPR spectra, one can estimate the composition, spatial distribution, and local concentration of spins in the system under study. Earlier, it was shown[47,48] that the spectral components of paramagnetic centers stabilized in conjugated polymers and/or photoinitiated in their composites can be additionally broadened due to the weak anisotropy of the g-factor of spin charge carriers chaotically distributed in their bulk. The spectra of these systems can be also broadened due to the exchange coupling of polarons diffusing along polymer chains with immobilized spin charge carriers. Such effect was found in the study of various conjugated polymer[75−82] and polymer:fullerene[47,49,83−85] multispin nanocomposites. In this case, the probability of collision of paramagnetic centers with the equal spins $S = {}^1/_2$ should be determined by their spatial distribution and diffusion rate of polarons along the polymer chains,[75,86]

$$p_{ss} = \frac{1}{2} \times \frac{\alpha^2}{1 + \alpha^2} \tag{2}$$

where $\alpha = 3J_{ex}L^2/2\hbar\omega_{hop}$, J_{ex} is the constant of spin exchange interaction, L is a number of copolymer units along which a polaron spin is delocalized, $\hbar = h/2\pi$ is the Planck quantum constant, and $\omega_{hop} = \omega^0_{hop} \exp(E_a/k_BT)$ is the rate of spin Q1D hopping along polymer chain with the activation energy E_a. The spin delocalization factor L was determined to be 14−15 C−C units in *trans*-polyacetylene,[87,88] 10−13 thiophene rings in regioregular P3AT,[43,89,90] 6 pyrrole rings in polypyrrole,[91] 8−10 units in poly[2-methoxy-5-(3′,7′-dimethyloctyloxy)-1,4-phenylenevinylene] (MDMO-PPV),[43] 8−9 units in poly[2,5-dimethoxy-1,4-phenylene-1,2-ethenylene-2-methoxy-5-(2-ethylhexyloxy)(1,4-phenylene-1,2-ethenylene)] (M3EH-PPV),[92] and 3 units in PCDTBT.[20,48] The latter value was used for interpretation of spin coupling and dynamics in the copolymer composites under study. In this case, the line broadening should follow the law[75,86]

$$\delta(\Delta\omega) = p_{ss}\omega_{hop}n_j \tag{3}$$

where n_j is the number of counter spins per each copolymer unit. The exchange interaction of charge carriers in various multispin systems can vary over a wide range. In the case of a weak/strong spin exchange, an increase in the Q1D mobility of the polarons should lead to a decrease/increase in the rate of radical exchange and to a respective narrowing/broadening of the signal line. This often initiates extreme changes in spin-dependent processes occurring in polymer semiconductors and their composites.[47,79,80]

In Figure 5 are shown the temperature dependences of line widths of the polarons, ΔB^P_{PP}, and methanofullerene radical anions, ΔB^{mF}_{PP}, photoinitiated in BHJ of the studied composites with achromatic, white light with a CCT of 5500 K. The data presented in the Figure evidence that the ΔB^{mF}_{PP} value determined for all the composites, varies little over the entire temperature range. This conclusion is also valid for polarons photoinitiated in the F8T2:PC_{61}BM and PCDTBT:PC_{61}BM systems. At the same time, polarons photoinitiated in the PFO−DBT:PC_{61}BM composite are characterized by an extreme change in the corresponding parameter ΔB^P_{PP} with a characteristic temperature $T_c \approx 120$ K. Such an effect can be due to a stronger exchange of polarons diffusing with energy activation $E_0 = 0.042_8$ eV, with other paramagnetic centers due to specific structural and morphological features of this sample. The additional broadening of the LEPR spectra due to spin relaxation and diffusion is discussed below.

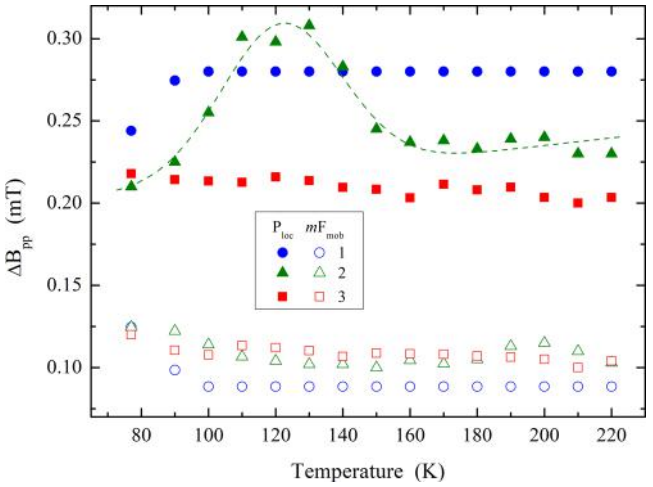

Figure 5. Temperature dependences of the peak-to peak line width of polarons ΔB^P_{PP} and methanofullerene radical anions ΔB^{mF}_{PP} (filled and open triangles, respectively) photoinitiated in the F8T2:PC_{61}BM (1), PFO−DBT:PC_{61}BM (2), and PCDTBT:PC_{61}BM (3) composites by by achromatic, white light source with CCT of T_c = 5500 K. The dashed line shows the dependence calculated from 2 with $\omega^0_{hop} = 1.1 \times 10^8$ s^{-1} and $E_0 = 0.042_8$ eV.

3.6. Spin Relaxation and Dynamics. Spin relaxation is one more important parameter reflecting all spin-assisted processes occurring in the systems under study. Analyzing parameters of such process, it become possible to clear the interaction of a solitary charge carriers with own microenvironment and other spin ensembles which can change the direction of spin precession during the characteristic times of spin−lattice and spin−spin relaxation, T_1 and T_2, respectively.

When the magnetic term B_1 of microwave field reaches a certain critical value in the EPR cavity, spectral lines of spin reservoirs begin to broaden and to increase nonlinearly with B_1 due to their steady-state microwave saturation,[57] as happens in the other solids.[56] At first, this effect is registered in the low-field contribution of polarons captured by deep traps and then in the spectrum attributed to the methanofullerene radical anions. The difference in microwave saturation and in g-factors of the polymer and fullerene moiety allows separately determining their effective relaxation parameters. Earlier, it

DOI: 10.1021/acs.jpcc.9b03402
J. Phys. Chem. C 2019, 123, 16533−16545

was shown[51−54] that these parameters of both charge carriers depend not only on the structure of a copolymer composite but also on the energy of the initiated photons $h\nu_{ph}$. They should also reflect spin interaction with other spin ensembles and environmental lattice phonons.

Temperature dependences of relaxation times determined for the polarons and methanofullerene radical anions upon steady-state illumination of the composites under study are shown in Figure 6. It is seen from the figure that the spin−spin

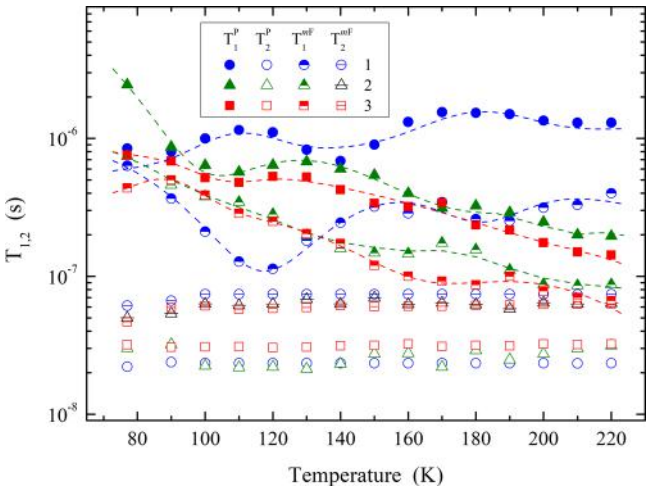

Figure 6. Temperature dependences of spin−lattice, T_1, and spin−spin, T_2, relaxation times of polarons $P^{+\bullet}$ (filled and open points, respectively) and methanofullerene radical anions $mF^{-\bullet}$ (semifilled and crossed points, respectively) initiated in the F8T2:$PC_{61}BM$ (1), PFO−DBT:$PC_{61}BM$ (2), and PCDTBT:$PC_{61}BM$ (3) composites by achromatic white light sources with CCT of T_c = 5500 K. The error does not exceed the area of experimental points. The dashed lines are drawn arbitrarily only for illustration to guide the eye.

relaxation time of both the charge carriers in all the systems are characterized by weak temperature dependences. On the other hand, the polarons demonstrate more complex dependences and besides T_1 obtained for these charge carriers exceeds that determined for the opposite ones in all composites studied. This cannot be originated from electron-transfer mechanism. Boltzmann distribution of phonons responsible for the spin−lattice relaxation cannot be too different in both spin charge carriers because both moieties consist of unsaturated carbon−carbon backbone with similar vibrational energies, so then an effective lattice temperature for both the spin ensembles is expected to be quite similar in such composites.[67] We can assume the change in morphology of the sample upon its heating. This changes the coupling and, consequently, effective electron relaxation of spin packets photoinitiated in the sample.[47,49] Respective parameters obtained for the samples under study irradiation by white light with different CCT are also summarized in Table 1.

The spin−lattice relaxation of both charge carriers photoinduced in the F8T2:$PC_{61}BM$ composite varies antibathically with a temperature with characteristic points near 110 and 180 K. The same parameters, obtained for the PFO−DBT:$PC_{61}BM$ and PCDTBT:$PC_{61}BM$ BHJ, mostly monotonously decrease with their heating. Such a difference can be explained by the proximity of the structures of the PFO−DBT:$PC_{61}BM$ and PCDTBT:$PC_{61}BM$ composites, as well as their greater ambipolarity compared with the F8T2:$PC_{61}BM$ one. This indicates that the variation in spin relaxation obtained for these systems are definitely originated from their ordered/disordered morphology balance in parallel with the interaction of charge carriers with different spin packets and their microenvironment. Besides this, an exchange interaction between these spin ensembles is modulated by spin−orbit coupling that depends on a sufficient density of vibrational and rotational states.[93] This accelerates electron relaxation of all spins stabilized or/and initiated in the system. Because the relaxation times have been measured over a wide temperature range, multiple relaxation mechanisms may simulate the data equally well. In order to distinguish between relaxation mechanisms, multifrequency EPR measurements may be appeared to be more efficient.[93] All the relaxation parameters obtained for all the composites under study are close to those determined by the cw EPR method for various conjugated polymers[36,37,94] and polymer:fullerene nanocomposites.[47,49]

Since the charge in the studied systems is transferred by spin carriers, the dimensionality of the system, as well as the number and diffusion rate of such carriers, has a significant impact on their relaxation times. Dissociation of the original excitons in Q1D polymer:fullerene systems first leads to the formation of radical pairs $P^{+\bullet}_{mob} \leftrightarrow mF^{-\bullet}_{mob}$. Part of these charge carriers fall into deep spin traps formed in the polymer matrix due to its disordering. The remaining carriers transfer charge along the polymer chains and between the polymer chains with diffusion coefficients D^P_{1D} and D^P_{3D}, respectively. The moving polarons induce at the location of other spin ensembles an additional magnetic field, which accelerates the electron and nuclear relaxation of the entire system. This is also facilitated by the libration dynamics of the fullerene radical anions with a correlation time τ_c. Taking into account the predominance of the dipole−dipole interaction between spins in organic conjugated polymers and their composites,[36,37,94,95] the dynamic parameters of both spin charge carriers in the copolymer composites studied can be separately determined from the following equations:[96]

$$T_1^{-1}(\omega) = \langle\omega^2\rangle[2J(\omega_e) + 8J(2\omega_e)] \quad (4)$$

$$T_2^{-1}(\omega) = \langle\omega^2\rangle[3J(0) + 5J(\omega_e) + 2J(2\omega_e)] \quad (5)$$

where $\langle\omega^2\rangle = {}^1/_{10}\gamma_e^4\hbar^2S(S+1)n\Sigma_{ij}$ is the constant of dipole spin interaction in powder sample with the total sum concentration $n = n_1 + n_2/\sqrt{2}$ of the localized (n_1) and mobile (n_2) spins per each copolymer unit, γ_e is the gyromagnetic ratio for an electron, Σ_{ij} is the lattice sum for powder, $J(\omega_e) = (2D^l_{1D}\omega_e)^{-1/2}$ at $D_{1D} \gg \omega_e \gg D^P_{3D}$ or $J(0) = (2D^l_{1D}D^P_{3D})^{-1/2}$ at $D_{1D} \gg \omega_e$ is a spectral density function for Q1D motion, and $D^l_{1D} = 4D^P_{1D}/L^2$.[36,37,97] Spin librations with correlation time τ_c are characterized by the another spectral density function $J(\omega_e) = 2\tau_c/(1 + \tau_c^2\omega_e^2)$.

The above spin dynamics parameters obtained for both the charge carriers photoinduced the F8T2:$PC_{61}BM$, PFO−DBT:$PC_{61}BM$, PCDTBT:$PC_{61}BM$ BHJ irradiation by achromatic light sources with different CCT at T = 77 K are presented in Table 1. Figure 7 shows how these parameters determined at CCT 5500 K change with the temperature. The data presented show that the rate of interchain charge transfer in the former system is weakly dependent on temperature, however, changes extremely at $T \approx 145$ K. The mobility of polarons along the chains of this composite also increases with the temperature, demonstrating extremity at $T \approx 120$ K. On

DOI: 10.1021/acs.jpcc.9b03402
J. Phys. Chem. C 2019, 123, 16533−16545

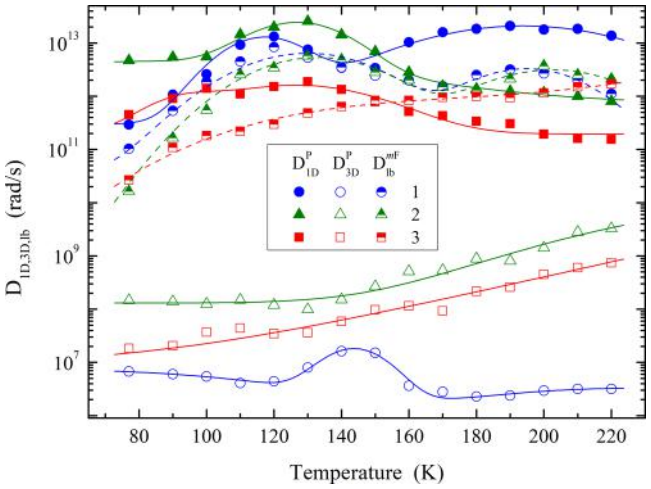

Figure 7. Translational intrachain, D^{P}_{1D} (filled points), hopping interchain, D^{P}_{3D} (open points) diffusion coefficients of polarons $P^{+\bullet}_{loc}$ and libration coefficient of methanofullerene radical anions, D^{mF}_{lb} (semifilled points), initiated in the F8T2:PC_{61}BM (1), PFO–DBT:PC_{61}BM (2), and PCDTBT:PC_{61}BM (3) composites by achromatic white light sources with CCT of T_c = 5500 K. The error does not exceed the area of experimental points. The solid and dashed lines are drawn arbitrarily only for illustration to guide the eye.

the other hand, the D^{P}_{3D} parameter of the PFO–DBT:PC_{61}BM and PCDTBT:PC_{61}BM composites monotonically increases with their heating (see Figure 7). Besides, the coefficient D^{P}_{1D} of polarons diffusing in these compounds also changes extremely at this temperature. Such dependences can be explained by the transition between ordered/crystalline and disordered/amorphous phases normally formed in conjugated polymers,[98] which changes their dimensionality, dynamics, and exchange coupling of charge carriers. The difference in the course of temperature dependences might indicate an increase in the ordering and effective dimensionality of the matrices of the compounds studied in the series F8T2:PC_{61}BM → PFO–DBT:PC_{61}BM → PCDTBT:PC_{61}BM. This also correlates with bandgap of the composites' backbones which determines their main electronic properties. The anisotropy $A = D^{P}_{1D}/D^{P}_{3D}$ of polaron diffusion in copolymer matrices of the above series first increases from 4.34×10^4 up to 3.19×10^6 and then decreases down to 2.46×10^4. It follows antibathically the respective distribution function of the trap energy described above. This feature may be due to the effect on the Q1D spin dynamics of the presence of spin traps in these composites with differently disordered ambipolar matrices.

IV. CONCLUSIONS

The obtained results evidence the advantages of the cw LEPR method in the study of the spin-assisted processes carried out in serial narrow-bandgap copolymer composites F8T2:PC_{61}BM, PFO–DBT:PC_{61}BM, and PCDTBT:PC_{61}BM with electron-withdrawing and electron-donating subunits. It was clearly demonstrated an expectable initiation of mobile positively charged polarons and negatively charged methanofullerene radical anions on adjacent layers upon their irradiation with near-infrared, visible, and ultraviolet light. A significant difference was found in the relaxation, dynamics, and interaction of these charge carriers with their microenvironment. Some of these carriers transfer a charge through BHJ of composites to electrodes, while the main polarons are captured by deep spin traps formed in these systems due to their disordering. The formation in the composites of deep traps changes the energy levels of spin excitations, originates the dependence of the energy conversion efficiency on the spin state and the lattice phonon energy. Once the energy of the lattice phonons increases, some part of so immobilized polarons can be realized out of these traps subsequently recombine with oppositely charged charge carriers. So, the recombination process in the samples can be interpreted in terms of the multistep trapping-detrapping of polarons in their backbone. The charges in the F8T2:PC_{61}BM and PFO–DBT:PC_{61}BM composites recombine in terms of bimolecular, second order process, whereas geminate recombination in the PCDTBT:PC_{61}BM BHJ follows the first order. The introducing of the benzothiadiazole subgroup between the thiophene subgroups during the transition from F8T2 backbone to PFO–DBT one does not noticeably change the mechanism of carrier recombination in the corresponding composite. On the other hand, replacing the dioctylfluorene subgroup with a carbazole subgroup during the transition from PFO–DBT to PFOTBT significantly decreases the order of recombination of polarons with methanofullerene radical anions. Such a change in the mechanism of charge recombination can occur as a result of a variation in the composite ordering. The anisotropy of the polaron dynamics increases at the former transition by approximately 2 orders of magnitude and then decreases down at the PFO–DBT → PCDTBT replacement to the initial value. Such an effect may be originated due to the different ambipolarity of backbones of these copolymer composites. The sensitivity of the main parameters of charge carriers to their interaction with the other spin ensembles or/and lattice phonons can be used to create elements of molecular electronics and spintronics with spin-assisted characteristics. Because polarons and methanofullerene-radical anions act as intrachain and interlayer nanoscopic spin probes, respectively, the methodology described provides the opportunity for direct and easy screening in details of spin-assisted electronic processes carrying out in analogous organic multispin polymer systems.

AUTHOR INFORMATION

Corresponding Author

*(V.I.K.) E-mail: kivirus@gmail.com. Telephone: +7(496-52) 21882. Website: http://hf-epr.awardspace.us.

ORCID

Victor I. Krinichnyi: 0000-0002-5227-763X

Notes

The authors declare no competing financial interest.

ACKNOWLEDGMENTS

The reported study was in part funded by the Russian Foundation for Basic Research according to Research Project No 18-29-20011.

REFERENCES

(1) Vardeny, Z. V. *Organic Spintronics*. CRC Press: Boca Raton, 2010;.

(2) Xu, Y.; Awschalom, D. D.; Nitta, J. *Handbook of Spintronics*. Springer-Verlag: 2015.

(3) Sattler, K. D. *Handbook of Nanophysics: Nanoelectronics and Nanophotonics*. CRC Press: Boca Raton, 2010.

(4) Milichko, V. A.; Makarov, S. V.; Yulin, A. V.; Vinogradov, A. V.; Krasilin, A. A.; Ushakova, E.; Dzyuba, V. P.; Hey-Hawkins, E.; Pidko,

DOI: 10.1021/acs.jpcc.9b03402
J. Phys. Chem. C 2019, 123, 16533–16545

E. A.; Belov, P. A. Van Der Waals Metal-Organic Framework as an Excitonic Material for Advanced Photonics. *Adv. Mater.* **2017**, *29*, 1606034.
(5) Abobeih, M. H.; Cramer, J.; Bakker, M. A.; Kalb, N.; Twitchen, D. J.; Markham, M.; Taminiau, T. H. One-Second Coherence for a Single Electron Spin Coupled to a Multi-Qubit Nuclear-Spin Environment. *Nat. Commun.* **2018**, *9*, 2552.
(6) Tumbleston, J. R.; Collins, B. A.; Yang, L.; Stuart, A. C.; Gann, E.; Ma, W.; You, W.; Ade, H. The Influence of Molecular Orientation on Organic Bulk Heterojunction Solar Cells. *Nat. Photonics* **2014**, *8*, 385−391.
(7) Micadei, K.; Peterson, J. P. S.; Souza, A. M.; Sarthour, R. S.; Oliveira, I. S.; Landi, G. T.; Batalhão, T. B.; Serra, R. M.; Lutz, E., Reversing the Thermodynamic Arrow of Time Using Quantum Correlations. *arXiv:1711.03323 [quant-ph]* 2017.
(8) Hasan, T.; Sun, Z. P.; Wang, F. Q.; Bonaccorso, F.; Tan, P. H.; Rozhin, A. G.; Ferrari, A. C. Nanotube-Polymer Composites for Ultrafast Photonics. *Adv. Mater.* **2009**, *21*, 3874−3899.
(9) Bonaccorso, F.; Sun, Z.; Hasan, T.; Ferrari, A. C. Graphene Photonics and Optoelectronics. *Nat. Photonics* **2010**, *4*, 611−622.
(10) Heeger, A. J. Semiconducting Polymers: The Third Generation. *Chem. Soc. Rev.* **2010**, *39*, 2354−2371.
(11) Yonezawa, K.; Ito, M.; Kamioka, H.; Yasuda, T.; Han, L. Y.; Moritomo, Y. Charge-Transfer State and Charge Dynamics in Poly(9,9 '-Dioctylfluorene-Co-Bithiophene) and 6,6 -Phenyl C-70-Butyric Acid Methyl Ester Blend Film. *Appl. Phys. Express* **2011**, *4*, 122601.
(12) Gmucová, K.; Nádaždy, V.; Váry, T. Density of Dark and Light-Induced Polaron States in Polymer PFO and Copolymer PFO-DBT Thin Films. *AIP Conf. Proc.* **2017**, *1996*, 020014.
(13) Hou, Q.; Xu, Y. S.; Yang, W.; Yuan, M.; Peng, J. B.; Cao, Y. Novel Red-Emitting Fluorene-Based Copolymers. *J. Mater. Chem.* **2002**, *12*, 2887−2892.
(14) Fan, S. W.; Sun, M. L.; Chen, Z.; Luo, J.; Hou, Q.; Peng, J. B.; Yang, H.; Zhang, D. Q.; Li, F. Y.; Cao, Y. Comparative Study on Polymer Light-Emitting Devices Based on Blends of Polyfluorene and 4,7-di-2-Thienyl-2,1,3-Benzothiadiazole with Devices Based on Copolymer of the Same Composition. *J. Phys. Chem. B* **2007**, *111*, 6113−6117.
(15) Park, S. H.; Roy, A.; Beaupre, S.; Cho, S.; Coates, N.; Moon, J. S.; Moses, D.; Leclerc, M.; Lee, K.; Heeger, A. J. Bulk Heterojunction Solar Cells with Internal Quantum Efficiency Approaching 100%. *Nat. Photonics* **2009**, *3*, 297−302.
(16) Li, G.; Zhu, R.; Yang, Y. Polymer Solar Cells. *Nat. Photonics* **2012**, *6*, 153−161.
(17) Seok, J.; Shin, T. J.; Park, S.; Cho, C.; Lee, J.-Y.; Yeol Ryu, D.; Kim, M. H.; Kim, K. Efficient Organic Photovoltaics Utilizing Nanoscale Heterojunctions in Sequentially Deposited Polymer/Fullerene Bilayer. *Sci. Rep.* **2015**, *5*, 8373.
(18) Tseng, H.-R.; Phan, H.; Luo, C.; Wang, M.; Perez, L. A.; Patel, S. N.; Ying, L.; Kramer, E. J.; Nguyen, T.-Q.; Bazan, G. C.; et al. High-Mobility Field-Effect Transistors Fabricated with Macroscopic Aligned Semiconducting Polymers. *Adv. Mater.* **2014**, *26*, 2993−2998.
(19) Moon, J. S.; Jo, J.; Heeger, A. J. Nanomorphology of PCDTBT:$PC_{70}BM$ Bulk Heterojunction Solar Cells. *Adv. Energy Mater.* **2012**, *2*, 304−308.
(20) Niklas, J.; Mardis, K. L.; Banks, B. P.; Grooms, G. M.; Sperlich, A.; Dyakonov, V.; Beaupré, S.; Leclerc, M.; Xu, T.; Yue, L.; et al. Highly-Efficient Charge Separation and Polaron Delocalization in Polymer−Fullerene Bulk-Heterojunctions: A Comparative Multi-Frequency EPR and DFT Study. *Phys. Chem. Chem. Phys.* **2013**, *15*, 9562−9574.
(21) Langer, F.; Schmid, C. P.; Schlauderer, S.; Gmitra, M.; Fabian, J.; Nagler, P.; Schuller, C.; Korn, T.; Hawkins, P. G.; Steiner, J. T.; et al. Lightwave Valleytronics in a Monolayer of Tungsten Diselenide. *Nature* **2018**, *557*, 76−80.
(22) Friend, R. H.; Gymer, R. W.; Holmes, A. B.; Burroughes, J. H.; Marks, R. N.; Taliani, C.; Bradley, D. D. C.; Dos Santos, D. A.; Brédas, J. L.; Logdlund, M.; et al. Electroluminescence in Conjugated Polymers. *Nature* **1999**, *397*, 121−128.
(23) Rocha, A. R.; García-suárez, V. M.; Bailey, S. W.; Lambert, C. J.; Ferrer, J.; Sanvito, S. Towards Molecular Spintronics. *Nat. Mater.* **2005**, *4*, 335−339.
(24) Dediu, V.; Hueso, L. E.; Bergenti, I.; Riminucci, A.; Borgatti, F.; Graziosi, P.; Newby, C.; Casoli, F.; De Jong, M. P.; Taliani, C.; et al. Room-Temperature Spintronic Effects in Alq3-Based Hybrid Devices. *Phys. Rev. B: Condens. Matter Mater. Phys.* **2008**, *78*, 115203.
(25) Zhang, X.; Steckler, T. T.; Dasari, R. R.; Ohira, S.; Potscavage, W. J.; Tiwari, S. P.; Coppee, S.; Ellinger, S.; Barlow, S.; Brédas, J.-L.; et al. Dithienopyrrole-Based Donor−Acceptor Copolymers: Low Band-Gap Materials for Charge Transport, Photovoltaics and Electrochromism. *J. Mater. Chem.* **2010**, *20*, 123−134.
(26) Yuen, J. D.; Fan, J.; Seifter, J.; Lim, B.; Hufschmid, R.; Heeger, A. J.; Wudl, F. High Performance Weak Donor-Acceptor Polymers in Thin Film Transistors: Effect of the Acceptor on Electronic Properties, Ambipolar Conductivity, Mobility, and Thermal Stability. *J. Am. Chem. Soc.* **2011**, *133*, 20799−20807.
(27) Gibson, G. L.; McCormick, T. M.; Seferos, D. S. Atomistic Band Gap Engineering in Donor-Acceptor Polymers. *J. Am. Chem. Soc.* **2012**, *134*, 539−547.
(28) Lupton, J. M.; McCamey, D. R.; Boehme, C. Coherent Spin Manipulation in Molecular Semiconductors: Getting a Handle on Organic Spintronics. *ChemPhysChem* **2010**, *11*, 3040−3058.
(29) Leo, K. Elementary Processes in Organic Photovoltaics. *Adv. Polym. Sci.* **2017**, *272*, 421.
(30) Yuen, J. D.; Wang, M.; Fan, J.; Sheberla, D.; Kemei, M.; Banerji, N.; Scarongella, M.; Valouch, S.; Pho, T.; Kumar, R.; et al. Importance of Unpaired Electrons in Organic Electronics. *J. Polym. Sci., Part A: Polym. Chem.* **2015**, *53*, 287−293.
(31) Tachiya, M.; Seki, K. Theory of Bulk Electron-Hole Recombination in a Medium with Energetic Disorder. *Phys. Rev. B: Condens. Matter Mater. Phys.* **2010**, *82*, 085201.
(32) Lukina, E. A.; Uvarov, M. N.; Kulik, L. V. Charge Recombination in P3HT/$PC_{70}BM$ Composite Studied by Light-Induced EPR. *J. Phys. Chem. C* **2014**, *118*, 18307−18314.
(33) Engel, H. A.; Recher, P.; Loss, D. Electron Spins in Quantum Dots for Spintronics and Quantum Computation. *Solid State Commun.* **2001**, *119*, 229−236.
(34) Schweiger, A.; Jeschke, G. *Principles of Pulse Electron Paramagnetic Resonance*; Oxford University Press: Oxford, 2001.
(35) Davidov, D.; Moraes, F.; Heeger, A. J.; Wudl, F.; Kim, H.; Dalton, L. R. Electron-Spin Echo Modulation and Relaxation in Polythiophene. *Solid State Commun.* **1985**, *53*, 497−500.
(36) Mizoguchi, K. Spin Dynamics Study in Conducting Polymers by Magnetic-Resonance. *Jpn. J. Appl. Phys. Part 1* **1995**, *34*, 1−19.
(37) Mizoguchi, K.; Kuroda, S., Magnetic Properties of Conducting Polymers. In *Handbook of Organic Conductive Molecules and Polymers*, Nalwa, H. S., Ed. John Wiley & Sons: Chichester, NY, 1997; Vol. 3, pp 251−317.
(38) Uvarov, M. N.; Kulik, L. V. Electron Spin Echo of Photoinduced Spin-Correlated Polaron Pairs in P3ht:Pcbm Composite. *Appl. Magn. Reson.* **2013**, *44*, 97−106.
(39) Kraffert, F.; Steyrleuthner, R.; Albrecht, S.; Neher, D.; Scharber, M. C.; Bittl, R.; Behrends, J. Charge Separation in Pcpdtbt:Pcbm Blends from an EPR Perspective. *J. Phys. Chem. C* **2014**, *118*, 28482−28493.
(40) Misra, S. K. *Multifrequency Electron Paramagnetic Resonance. Theory and Applications*. Wiley-VCH: Weinheim, 2011; Vol. 2.
(41) Liedtke, M.; Sperlich, A.; Kraus, H.; Baumann, A.; Deibel, C.; Wirix, M. J. M.; Loos, J.; Cardona, C. M.; Dyakonov, V. Triplet Exciton Generation in Bulk-Heterojunction Solar Cells Based on Endohedral Fullerenes. *J. Am. Chem. Soc.* **2011**, *133*, 9088−9094.
(42) Naveed, K.-u.-R.; Wang, L.; Yu, H.; Ullah, R. S.; Haroon, M.; Fahad, S.; Li, J.; Elshaarani, T.; Khan, R. U.; Nazir, A. Recent Progress in the Electron Paramagnetic Resonance Study of Polymers. *Polym. Chem.* **2018**, *9*, 3306−3335.

DOI: 10.1021/acs.jpcc.9b03402
J. Phys. Chem. C 2019, 123, 16533−16545

(43) Aguirre, A.; Gast, P.; Orlinskii, S.; Akimoto, I.; Groenen, E. J. J.; El Mkami, H.; Goovaerts, E.; Van Doorslaer, S. Multifrequency EPR Analysis of the Positive Polaron in I_2-Doped Poly(3-hexylthiophene) and in Poly[2-methoxy-5-(3,7-dimethyloctyloxy)]-1,4-phenylenevinylene. *Phys. Chem. Chem. Phys.* **2008**, *10*, 7129−7138.
(44) Poluektov, O. G.; Filippone, S.; Martín, N.; Sperlich, A.; Deibel, C.; Dyakonov, V. Spin Signatures of Photogenerated Radical Anions in Polymer-[70]Fullerene Bulk Heterojunctions: High Frequency Pulsed EPR Spectroscopy. *J. Phys. Chem. B* **2010**, *114*, 14426−14429.
(45) Konkin, A.; Ritter, U.; Scharff, P.; Mamin, G.; Aganov, A.; Orlinskii, S.; Krinichnyi, V. I.; Egbe, D. A. M.; Ecke, G.; Romanus, H. Multifrequency X-, W-Band ESR Study on Photo-Induced Ion Radical Formation in Solid Films of Mono- and Di-Fullerenes Embedded in Conjugated Polymers. *Carbon* **2014**, *77*, 11−17.
(46) Ledwon, P.; Thomson, N.; Angioni, E.; Findlay, N. J.; Skabara, P. J.; Domagala, W. The Role of Structural and Electronic Factors in Shaping the Ambipolar Properties of Donor − Acceptor Polymers of Thiophene and Benzothiadiazole. *RSC Adv.* **2015**, *5*, 77303−77315.
(47) Krinichnyi, V. I. EPR Spectroscopy of Polymer:Fullerene Nanocomposites. *Spectroscopy of Polymer Nanocomposites* **2016**, 202−275.
(48) Niklas, J.; Poluektov, O. G. Charge Transfer Processes in OPV Materials as Revealed by EPR Spectroscopy. *Adv. Energy Mater.* **2017**, *7*, 1602226.
(49) Krinichnyi, V. I., EPR Spectroscopy of Polarons in Conjugated Polymers and Their Nanocomposites. In *Polarons: Recent Progress and Perspectives*, Laref, A., Ed. Nova Science Publishers, Inc.: Hauppauge, NY, 2018; pp 1−105.
(50) Krinichnyi, V. I.; Yudanova, E. I.; Denisov, N. N. The Role of Spin Exchange in Charge Transfer in Low-Bandgap Polymer:-Fullerene Bulk Heterojunctions. *J. Chem. Phys.* **2014**, *141*, 044906.
(51) Krinichnyi, V. I.; Yudanova, E. I.; Bogatyrenko, V. R. Effect of Spin Traps on Charge Transport in Low-Bandgap Copolymer:Fullerene Composites. *J. Phys. Chem. Solids* **2017**, *111*, 153−159.
(52) Krinichnyi, V. I.; Yudanova, E. I.; Bogatyrenko, V. R. Effect of Spin Localization on Charge Transport in Low-Bandgap Bilayered Ordered Nanocomposites. *Sol. Energy Mater. Sol. Cells* **2018**, *174*, 333−341.
(53) Krinichnyi, V. I.; Yudanova, E. I.; Bogatyrenko, V. R. Light-Induced EPR Study of Spin-Assisted Charge Transport in PFOT:PC_{61}BM Composite. *J. Photochem. Photobiol., A* **2019**, *372*, 288−295.
(54) Yudanova, E. I.; Krinichnyi, V. I.; Bogatyrenko, V. R.; Denisov, N. N.; Nazarov, D. I. Influence of Photogeneration Frequency on the Transport of Spin Charge Carriers in the Copolymer−Methanofullerene Composite: EPR Study. *High Energy Chem.* **2019**, *53*, 219−227.
(55) Krzystek, J.; Sienkiewicz, A.; Pardi, L.; Brunel, L. C. DPPH as a Standard for High-Field EPR. *J. Magn. Reson.* **1997**, *125*, 207−211.
(56) Weil, J. A.; Bolton, J. R.; Wertz, J. E. *Electron Paramagnetic Resonance: Elementary Theory and Practical Applications*; Wiley-Interscience: New York, 2007; Vol. *2d*.
(57) Marumoto, K.; Takeuchi, N.; Ozaki, T.; Kuroda, S. ESR Studies of Photogenerated Polarons in Regioregular Poly(3-Alkylthiophene)-Fullerene Composite. *Synth. Met.* **2002**, *129*, 239−247.
(58) Huang, J. H.; Lee, C. P.; Ho, Z. Y.; Kekuda, D.; Chu, C. W.; Ho, K. C. Enhanced Spectral Response in Polymer Bulk Heterojunction Solar Cells by Using Active Materials with Complementary Spectra. *Sol. Energy Mater. Sol. Cells* **2010**, *94*, 22−28.
(59) Gunduz, B. Controlling of Spectral and Optical Parameters of the F8T2 Liquid-Crystalline Polymer (LCP) by Molarity for Optoelectronic Devices. *Optik* **2015**, *126*, 4566−4573.
(60) Huang, J. H.; Yang, C. Y.; Ho, Z. Y.; Kekuda, D.; Wu, M. C.; Chien, F. C.; Chen, P. L.; Chu, C. W.; Ho, K. C. Annealing Effect of Polymer Bulk Heterojunction Solar Cells Based on Polyfluorene and Fullerene Blend. *Org. Electron.* **2009**, *10*, 27−33.
(61) Hare, J. P.; Kroto, H. W.; Taylor, R. Preparation and UV/Visible Spectra of Fullerenes C60 and C70. *Chem. Phys. Lett.* **1991**, *177*, 394−398.
(62) Lim, E.; Jung, B.-J.; Chikamatsu, M.; Azumi, R.; Yoshida, Y.; Yase, K.; Do, L.-M.; Shim, H.-K. Doping Effect of Solution-Processed Thin-Film Transistors Based on Polyfluorene. *J. Mater. Chem.* **2007**, *17*, 1416−1420.
(63) Zhou, Q. M.; Hou, Q.; Zheng, L. P.; Deng, X. Y.; Yu, G.; Cao, Y. Fluorene-Based Low Band-Gap Copolymers for High Performance Photovoltaic Devices. *Appl. Phys. Lett.* **2004**, *84*, 1653−1655.
(64) Fakir, M. S.; Supangat, A.; Sulaiman, K. Fabrication of PFO-DBT:OXCBA Nanostructured Composite via Hard Template. *J. Appl. Polym. Sci.* **2016**, *133*, 44228.
(65) Saitoh, L.; Babu, R. R.; Kannappan, S.; Kojima, K.; Mizutani, T.; Ochiai, S. Performance of Spray Deposited Poly]N-9 ”-Hepta-Decanyl-2,7-Carbazole-alt-5, 5-(4 ’,7 ’-di-2-Thieny1−2 ’,1 ’,3 ’-Benzothiadiazole)] /[6,6] -Phenyl-C61-Butyric Acid Methyl Ester Blend Active Layer Based Bulk Heterojunction Organic Solar Cell Devices. *Thin Solid Films* **2012**, *520*, 3111−3117.
(66) Wang, S.-f.; Liu, Y.-n.; Yang, J.; Tao, Y.-t.; Guo, Y.; Cao, X.-d.; Zhang, Z.-g.; Li, Y.-f.; Huang, W. Orthogonal Solubility in Fully Conjugated Donor-Acceptor Block Copolymers: Compatibilizers for Polymer/Fullerene Bulk-Heterojunction Solar Cells. *Chin. J. Polym. Sci.* **2017**, *35*, 207−218.
(67) Dyakonov, V.; Zoriniants, G.; Scharber, M.; Brabec, C. J.; Janssen, R. A. J.; Hummelen, J. C.; Sariciftci, N. S. Photoinduced Charge Carriers in Conjugated Polymer-Fullerene Composites Studied with Light-Induced Electron-Spin Resonance. *Phys. Rev. B: Condens. Matter Mater. Phys.* **1999**, *59*, 8019−8025.
(68) Baleg, A. A.; Masikini, M.; John, S. V.; Williams, A. R.; Jahed, N.; Baker, P.; Iwuoha, E. Conducting Polymers and Composites. *Functional Polymers* **2018**, 1−54.
(69) Krinichnyi, V. I.; Yudanova, E. I.; Denisov, N. N. Light-Induced EPR Study of Charge Transfer in Poly(3-Hexylthiophene)/Fullerene Bulk Heterojunction. *J. Chem. Phys.* **2009**, *131*, 044515.
(70) Konkin, A.; Ritter, U.; Scharff, P.; Roth, H.-K.; Aganov, A.; Sariciftci, N. S.; Egbe, D. A. M. Photo-Induced Charge Separation Process in (PCBM-C_{120}O)/(M3EH-PPV) Blend Solid Film Studied by Means of X- and K-Bands ESR at 77 and 120 K. *Synth. Met.* **2010**, *160*, 485−489.
(71) Kaufman, J. H.; Colaneri, N.; Scott, J. C.; Street, G. B. Evolution of Polaron States into Bipolarons in Polypyrrole. *Phys. Rev. Lett.* **1984**, *53*, 1005−1008.
(72) Čík, G.; Šeršeň, F.; Dlháň, L. Thermally Induced Transitions of Polarons to Bipolarons in Poly (3-Dodecylthiophene). *Synth. Met.* **2005**, *151*, 124−130.
(73) Griffin, J.; Pearson, A. J.; Scarratt, N. W.; Wang, T.; Dunbar, A. D. F.; Yi, H.; Iraqi, A.; Buckley, A. R.; Lidzey, D. G. Organic Photovoltaic Devices with Enhanced Efficiency Processed from Non-Halogenated Binary Solvent Blends. *Org. Electron.* **2015**, *21*, 216−222.
(74) Grant, W.; Strandberg, M. Statistical Theory of Spin-Spin Interactions in Solids. *Phys. Rev.* **1964**, *135*, A715−A726.
(75) Houze, E.; Nechtschein, M. ESR in Conducting Polymers: Oxygen-Induced Contribution to the Linewidth. *Phys. Rev. B: Condens. Matter Mater. Phys.* **1996**, *53*, 14309−14318.
(76) Kerimov, M. K. Spin Exchange in Iodine-Doped Polydiacetylene. *Phys. Solid State* **1999**, *41*, 1726−1728.
(77) Tipikin, D. S.; Earl, K. A.; Freed, J. H. The High-Frequency EPR Spectra of Polyaniline: Line Narrowing Due to the Spin Exchange. *Polymer Science, Ser. B* **1999**, *41*, 1043−1047.
(78) Krinichnyi, V. I.; Tokarev, S. V.; Roth, H. K.; Schrödner, M.; Wessling, B. Multifrequency EPR Study of Metal-Like Domains in Polyaniline. *Synth. Met.* **2005**, *152*, 165−168.
(79) Krinichnyi, V. I.; Roth, H. K.; Schrödner, M.; Wessling, B. EPR Study of Polyaniline Highly Doped by *p*-Toluenesulfonic Acid. *Polymer* **2006**, *47*, 7460−7468.
(80) Krinichnyi, V. I.; Yudanova, E. I.; Wessling, B. Influence of Spin−Spin Exchange on Charge Transfer in PANI-ES/P3DDT/PCBM Composite. *Synth. Met.* **2013**, *179*, 67−73.
(81) Krinichnyi, V. I. Dynamics of Spin Charge Carriers in Polyaniline. *Appl. Phys. Rev.* **2014**, *1*, 021305.

DOI: 10.1021/acs.jpcc.9b03402
J. Phys. Chem. C 2019, 123, 16533−16545

(82) Yudanova, E. I.; Bogatyrenko, V. R.; Krinichnyi, V. I. EPR Study of Spin Interactions in Poly(3-Dodecylthiophene):Fullerene/Polyaniline:*p*-Toluenesulfonic Acid Composite. *High Energy Chem.* **2016**, *50*, 127−133.
(83) Konkin, A.; Bounioux, C.; Ritter, U.; Scharff, P.; Katz, E. A.; Aganov, A.; Gobsch, G.; Hoppe, H.; Ecke, G.; Roth, H. K. ESR and LESR X-Band Study of Morphology and Charge Carrier Interaction in Blended P3HT-SWCNT and P3HT-PCBM-SWCNT Solid Thin Films. *Synth. Met.* **2011**, *161*, 2241−2248.
(84) Zhang, Y.; Gautam, B. R.; Basel, T. P.; Mascaro, D. J.; Vardeny, Z. V. Organic Bulk Heterojunction Solar Cells Enhanced by Spin Interaction. *Synth. Met.* **2013**, *173*, 2−9.
(85) Kraffert, F.; Behrends, J. Spin-Correlated Doublet Pairs as Intermediate States in Charge Separation Processes. *Mol. Phys.* **2017**, *115*, 2373−2386.
(86) Molin, Y. N.; Salikhov, K. M.; Zamaraev, K. I. *Spin Exchange* **1980**, *8*, 260.
(87) Heeger, A. J.; Kivelson, S.; Schrieffer, J. R.; Su, W. P. Solitons in Conducting Polymers. *Rev. Mod. Phys.* **1988**, *60*, 781−850.
(88) Krinichnyi, V. I.; Pelekh, A. E.; Tkachenko, L. I.; Kozub, G. I. Study of Anisotropic Spin Dynamics in Pristine *trans* -Polyacetylene by Means of 2-mm EPR Spectroscopy. *Synth. Met.* **1992**, *46*, 13−22.
(89) Marumoto, K.; Takeuchi, N.; Kuroda, S. Nanoscale Spatial Extent of Photogenerated Polarons in Regioregular Poly(3-Octylthiophene). *Chem. Phys. Lett.* **2003**, *382*, 541−546.
(90) Kuroda, S.; Marumoto, K.; Sakanaka, T.; Takeuchi, N.; Shimoi, Y.; Abe, S.; Kokubo, H.; Yamamoto, T. Electron-Nuclear Double-Resonance Observation of Spatial Extent of Polarons in Polythiophene and Poly(3-Alkylthiophene). *Chem. Phys. Lett.* **2007**, *435*, 273−277.
(91) Pelekh, A. E.; Goldenberg, L. M.; Krinichnyi, V. I. Study of Dopped Polypyrrole by the Spin Probe Method at 3-cm and 2-mm Waveband EPR. *Synth. Met.* **1991**, *44*, 205−211.
(92) Konkin, A.; Popov, A.; Ritter, U.; Orlinskii, S.; Mamin, G.; Aganov, A.; Konkin, A. A.; Scharff, P. Combined W-Band Light-Induced ESR/ENDOR/TRIPLE and DFT Study of PPV-Type/$PC_{61}BM$ Ion Radicals. *J. Phys. Chem. C* **2016**, *120*, 28905−28911.
(93) Eaton, G. R.; Eaton, S. S. Multifrequency Electron Spin-Relaxation Times. *Multifrequency Electron Paramagnetic Resonance. Theory and Applications* **2011**, 719−753.
(94) Krinichnyi, V. I. 2-mm Waveband Electron Paramagnetic Resonance Spectroscopy of Conducting Polymers (Review). *Synth. Met.* **2000**, *108*, 173−222.
(95) Krinichnyi, V. I.; Pelekh, A. E.; Tkachenko, L. I.; Kozub, G. I. Study of Spin Dynamics in *trans* -Polyacetylene at 2-mm Waveband EPR. *Synth. Met.* **1992**, *46*, 1−12.
(96) Carrington, F.; McLachlan, A. D. *Introduction to Magnetic Resonance with Application to Chemistry and Chemical Physics*; Harper & Row, Publishers: New York, Evanston, IL, and London, 1967, Chapter 12, p 266.
(97) Nechtschein, M., Electron Spin Dynamics. In *Handbook of Conducting Polymers*, Skotheim, T. A.; Elsenbaumer, R. L.; Reynolds, J. R., Eds.; Marcel Dekker: New York, 1997; pp 141−163.
(98) Schweizer, K. S. Order−Disorder Transitions of π-Conjugated Polymers in Condensed Phases. I. General Theory. *J. Chem. Phys.* **1986**, *85*, 1156−1175.

DOI: 10.1021/acs.jpcc.9b03402
J. Phys. Chem. C 2019, 123, 16533−16545